MNRAS 000, 1–7 (2019) Preprint 28 January 2020 Compiled using MNRAS LATEX style file v3.0

Searching for a dusty cometary belt around TRAPPIST-1 with ALMA

S. Marino[1]★, M. C. Wyatt[2], G. M. Kennedy[3], M. Kama[2], L. Matrà[4], A. H. M. J. Triaud[5] and Th. Henning[1]

[1]*Max Planck Institute for Astronomy, Königstuhl 17, 69117 Heidelberg, Germany*
[2]*Institute of Astronomy, University of Cambridge, Madingley Road, Cambridge CB3 0HA, UK*
[3]*Department of Physics, University of Warwick, Gibbet Hill Road, Coventry, CV4 7AL, UK*
[4]*Harvard-Smithsonian Center for Astrophysics, 60 Garden Street, Cambridge, MA 02138, USA*
[5]*School of Physics & Astronomy, University of Birmingham, Edgbaston, Birmingham, B152TT, UK*

Accepted XXX. Received YYY; in original form ZZZ

ABSTRACT

Low mass stars might offer today the best opportunities to detect and characterise planetary systems, especially those harbouring close-in low mass temperate planets. Among those stars, TRAPPIST-1 is exceptional since it has seven Earth-sized planets, of which three could sustain liquid water on their surfaces. Here we present new and deep ALMA observations of TRAPPIST-1 to look for an exo-Kuiper belt which can provide clues about the formation and architecture of this system. Our observations at 0.88 mm did not detect dust emission, but can place an upper limit of 23μJy if the belt is smaller than 4 au, and 0.15 mJy if resolved and 100 au in radius. These limits correspond to low dust masses of $\sim 10^{-5} - 10^{-2}$ $M_\oplus$, which are expected after 8 Gyr of collisional evolution unless the system was born with a > 20 $M_\oplus$ belt of 100 km-sized planetesimals beyond 40 au or suffered a dynamical instability. This 20 $M_\oplus$ mass upper limit is comparable to the combined mass in TRAPPIST-1 planets, thus it is possible that most of the available solid mass in this system was used to form the known planets. A similar analysis of the ALMA data on Proxima Cen leads us to conclude that a belt born with a mass $\gtrsim 1$ $M_\oplus$ in 100 km-sized planetesimals could explain its putative outer belt at 30 au. We recommend that future characterisations of debris discs around low mass stars should focus on nearby and young systems if possible.

Key words: circumstellar matter - planetary systems - planets and satellites: dynamical evolution and stability - techniques: interferometric - methods: numerical - stars: individual: TRAPPIST-1.

1 INTRODUCTION

In recent years, the study of planetary systems around low mass stars has received great attention. This is partly due to low mass planets being easier to detect via transits around low mass stars, but also because their occurrence rate is higher compared to planets around FGK stars (e.g. Mulders et al. 2015; Hardegree-Ullman et al. 2019). Moreover, because of the lower luminosity of M stars, close-in planets could harbour liquid water in these systems. One example of such systems is TRAPPIST-1, a M8 dwarf star at 12 pc hosting at least seven Earth-sized planets (Gillon et al. 2016, 2017; Luger et al. 2017), all within 0.06 au. Three of these planets lie at a distance from the star where long-lived liquid water could exist on their surfaces (O'Malley-James & Kaltenegger 2017), although constraints on the composition of these planets are still very uncertain despite major efforts (e.g. de Wit et al. 2016, 2018; Moran et al. 2018; Wakeford et al. 2019; Dorn et al. 2018; Grimm et al. 2018; Burdanov et al. 2019). The composition of these planets is highly dependent on how these planets formed. For example, if they formed in situ these planets might be water poor (e.g. Hansen & Murray 2012), while if they formed further out and migrated in, as suggested by the near-resonant chain, then these planets might contain significant amounts of wa-

★ E-mail: sebastian.marino.estay@gmail.com

ter (e.g. Cresswell & Nelson 2006; Terquem & Papaloizou 2007; Ormel et al. 2017; Schoonenberg et al. 2019).

Moreover, volatile delivery through impacts of icy material formed further out (e.g. Marino et al. 2018; Kral et al. 2018; Schwarz et al. 2018; Dencs & Regály 2019) could also affect the composition of their atmospheres and surfaces. How much icy material lies exterior to a planetary system can be constrained by infrared observations which are sensitive to circumstellar dust that is continually replenished through the collisional break up of km-sized planetesimals (i.e. debris discs, see reviews by Wyatt 2008; Krivov 2010; Hughes et al. 2018). Thanks to Spitzer and Herschel, we know that at least 20% of A–K type stars host exo-Kuiper belts that are orders of magnitude brighter (and likely more massive) than the Kuiper belt (Eiroa et al. 2013; Matthews et al. 2014; Montesinos et al. 2016; Sibthorpe et al. 2018). However, the constraints on planetesimal discs around M type stars are poorer due to several factors, including small grain removal processes (Plavchan et al. 2005) and observational biases and low sensitivity (e.g. Wyatt 2008; Lestrade et al. 2009; Binks & Jeffries 2017; Kennedy et al. 2018).

Thanks to ALMA's unprecedented sensitivity at sub-mm wavelengths, it is now possible to search for planetesimal discs around low mass stars at greater depth, and constrain the architecture of planetary systems around low mass stars. In this paper we report deep ALMA observations of TRAPPIST-1. While previous to our observations there was no evidence for the presence of dust around TRAPPIST-1, the efficient planet formation in this system, its potentially young age (highly unconstrained until recently) and its proximity made it an ideal target to look for a planetesimal belt. This paper is organised as follows. In §2 we describe the ALMA observations and place upper limits on dust emission levels. Then, in §3 we compare these dust upper limits with collisional evolution models. Finally, in §4 we summarise our results and conclusions.

2 ALMA OBSERVATIONS

We observed TRAPPIST-1 using ALMA band 7 (0.88 mm) as part of the project 2017.1.00215.S (PI: S. Marino). The observations were split into 6 blocks that were executed between 3 May 2018 and 20 August 2018, with a total time on source of 4.5 h. Observations were taken using a total of 44–48 antennas, with baselines ranging between 35 and 240 m ($5^{\rm th}$ and $80^{\rm th}$ percentiles), which allows to recover structure on angular scales ranging between 0.″37 and 5″ (4.6 and 62 au projected in the sky). The average PWV ranged between 0.4 and 0.7 between the 6 blocks. The spectral setup was divided into 4 windows to observe the continuum, centred at 334.6, 336.5, 348.5 and 346.6 GHz. The first three had a total bandwidth of 2 GHz and a channel width of 15,625 kHz, while the latter a total bandwidth of 1.875 GHz and a channel width of 488.281 kHz (effective spectral resolution of 0.845 km s^{-1}) to look for CO 3-2 line emission. Finally, the observations were calibrated using CASA and the standard pipeline provided by ALMA.

We image the continuum with the task tclean in CASA, using natural weights to produce a reconstructed image with the lowest possible noise. Figure 1 presents the clean image, corrected by the primary beam and with a noise level or rms of 7.7 μJy beam^{-1} at the center. We do not find any emission arising from circumstellar material around TRAPPIST-1. The only detected source ($> 5\sigma$) is a marginally resolved object with a total flux 0.8 mJy that is likely sub-mm galaxy given ALMA number counts (we expect ~ 0.3 sources within the primary beam with a flux equal or larger than 0.8 mJy, Simpson et al. 2015; Carniani et al. 2015; Aravena et al. 2016). We also search for extended emission from an edge-on disk by computing the flux in a rectangular aperture centred on the star of width 1.5×beam (since we assume an edge-on disc co-planar with TRAPPIST-1 b–h) and variable length and position angle; no $> 3\sigma$ detection was found.

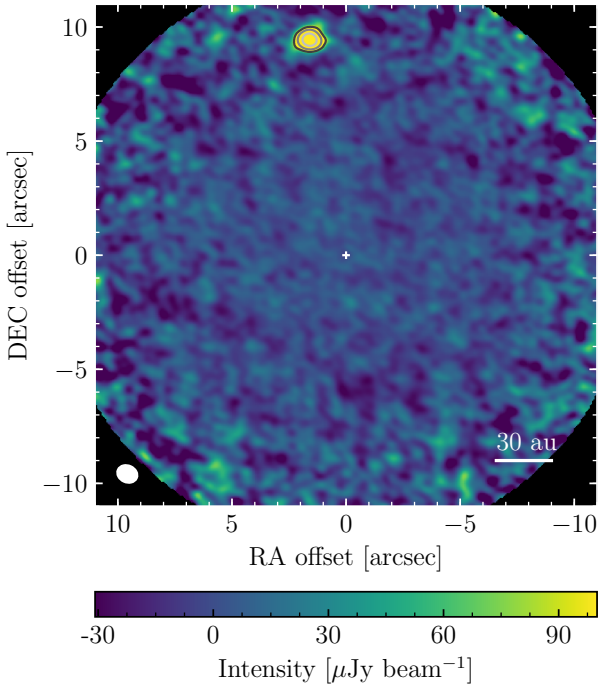

Figure 1. ALMA band 7 (0.88 mm) continuum image obtained with clean using natural weights. The beam size is 0.″71×0.″54 and has a PA of 65 deg. The image rms is 7.7 μJy beam^{-1}. The beam size is represented by a white ellipse on the bottom left corner. The black regions at the edges of the image represent where the sensitivity drops below 20% of that at the image center. The grey contours show emission above 5, 10 and 20 times the rms level.

We use the clean image to derive an upper limit on the 0.88 mm flux from any hidden dust in the system below our detection threshold. For an unresolved disc with a radius smaller than 4 au, we obtain a 3σ limit of 23 μJy. A planetesimal belt in the system could be larger and resolved. For this case we derive a flux upper limit by estimating the integrated flux uncertainty over a rectangular aperture centred on the star as described above, also taking into account the number of beams in this area and how the noise level increases away from the phase center. This leads to a flux upper limit that increases as a function of the disc diameter or aperture size, e.g. we find an upper limit of 150 μJy if it has an outer radius of 100 au. These flux upper limits can be converted to an upper limit on the disc fractional luminosity as a function of radius as shown in Figure 2. For this, we assume the dust has blackbody equilibrium temperatures $T_{\rm BB}(r) = 42(r/1\ {\rm au})^{-1/2}$ ($L_\star = 5.2\times10^{-4}\ L_\odot$, Filippazzo et al.

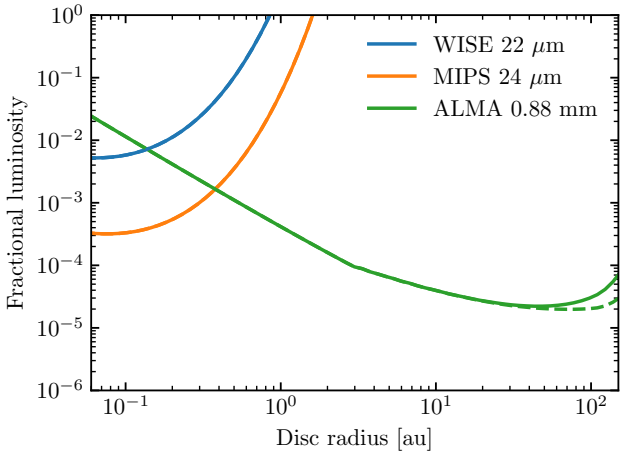

Figure 2. Upper limits on the fractional luminosity of a debris disc around TRAPPIST-1 based on WISE 22 μm (blue), MIPS 24 μm (orange) and ALMA 0.88 mm (green) data, assuming blackbody equilibrium temperatures (continuous lines). The dashed line represents the corrected limit by considering also the ISRF when calculating the equilibrium dust temperatures. Both green lines assume an edge-on disc orientation.

2015) and an opacity that declines with wavelength as $1/\lambda$ beyond 200 μm (Wyatt 2008). In the same figure we also overlay in blue the upper limit derived from WISE 22 μm (3 mJy, Wright et al. 2010) and MIPS 24 μm observations (0.2 mJy, which are limited by calibration uncertainties of $\sim$ 5%, Gautier et al. 2007). We find that the ALMA limit is significantly more constraining than the WISE and MIPS limit beyond 0.4 au. This is due to its high sensitivity and the longer wavelength, being more sensitive to cold dust. Based on our new observations we can rule out a debris disc with fractional luminosity higher than $\sim 2\times10^{-5}$ at a radius between 10–100 au.

Note that assuming blackbody equilibrium temperatures only based on the stellar radiation might not be a good assumption since the interstellar radiation field (ISRF) could contribute significantly to the radiation field at tens of au. In order to take this into account, we calculate the dust temperature as $(T^4_{\rm BB}(r) + T^4_{\rm ISRF})^{1/4}$, where $T_{\rm ISRF}$ is a fixed equilibrium temperature due to the ISRF. The equilibrium temperature of grains in the diffuse interstellar medium has been studied extensively (e.g. Li & Draine 2001), finding temperatures in the range 10–20 K for dust grains smaller than 1 μm, significantly higher than the blackbody equilibrium temperature of 3.6 K (obtained by integrating the analytic expressions presented by Mezger et al. 1982; Mathis et al. 1983). Larger grains, however, have lower temperatures close to blackbody since they have almost constant opacities at short wavelengths that dominate the ISRF. We thus assume $T_{\rm ISRF}$ = 3.6 K and incorporate this lower bound for dust temperatures to all calculations in §3. The green dashed line in Figure 2 is the corrected upper limit when taking into account the ISRF.

We also look for any CO 3-2 line emission, which also led to a non-detection. The achieved rms per 0.42 km s^{-1} channel is 0.5 mJy beam^{-1}. Therefore we can set a 3σ upper limit of 6 mJy km s^{-1} for any unresolved CO 3-2 emission interior

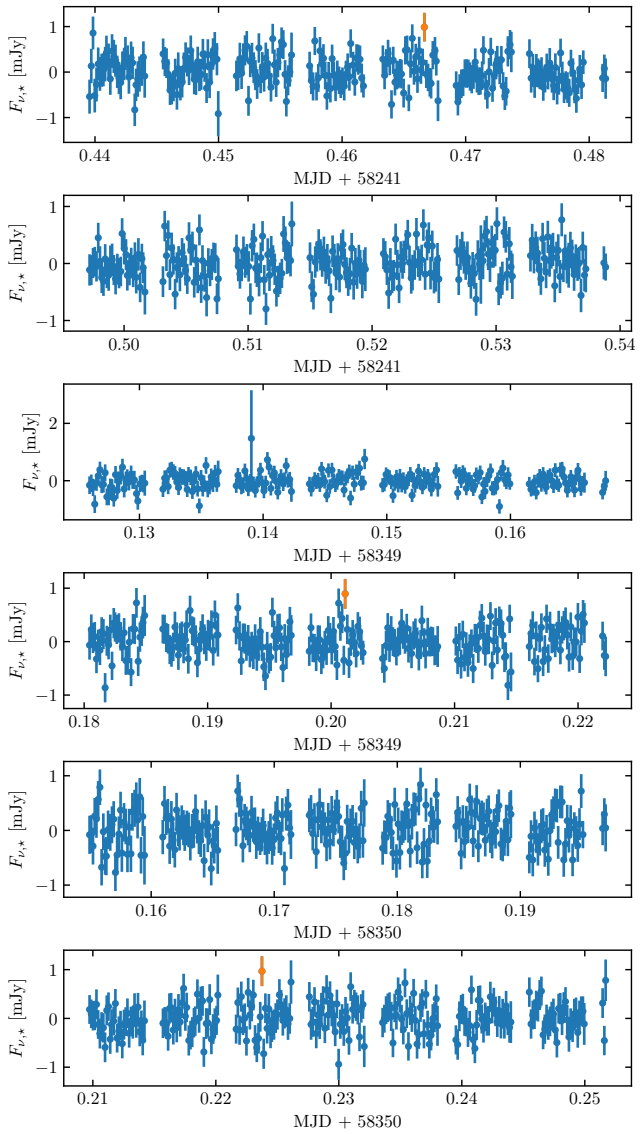

Figure 3. Measured flux at TRAPPIST-1 location vs time, integrated over 12s windows. Data points above 3σ are displayed in orange.

to 4 au and with a maximum Doppler shift of 10 km s^{-1} (i.e. beyond 1 au if in Keplerian rotation). Using the non-LTE tool by Matrà et al. (2018a) we translate this upper limit to a CO gas mass of $\sim 2\times10^{-8}$ $M_\oplus$.

Because low mass stars can have strong and highly variable emission at mm to cm wavelengths due to flaring activity, we also search for unresolved variable emission at the stellar position by imaging the data in time intervals of 12s. In Figure 3 we show the measured flux at the stellar position. We do not find any significant variable emission above the noise level (rms of 0.23 mJy over 12s window) that could arise from flares (as in Proxima Cen, MacGregor et al. 2018). We only find three single 3σ peaks over 1400 data points which is roughly consistent with the expected number of false positives for a normal distribution. The non-detection of variable emission from TRAPPIST-1 is consistent with

results reported by Hughes et al. (2019) which did not detect any emission at 3 mm with ALMA nor at 7 mm with the VLA for TRAPPIST-1. Note that the limits presented here at 0.88 mm are still consistent with flaring levels similar to Proxima Cen when taking into account the integration length and larger distance to TRAPPIST-1.

3 DISCUSSION

In this section we aim to constrain what initial planetesimal belt properties are still consistent with the observational limits and what we can rule-out. We do this by comparing a collisional evolution model to our non-detection of a debris disc around TRAPPIST-1 (§3.1) and to archival ALMA observations of Proxima Cen (§3.2).

We use the same collisional evolution model that has been used to fit observations of resolved debris discs (Wyatt et al. 2011; Marino et al. 2017). This model solves the evolution of the size distribution of solids in a collisional cascade, and here we assume the following:

(i) a maximum planetesimal size of 100 km,
(ii) size dependent strengths (Benz & Asphaug 1999; Stewart & Leinhardt 2009),
(iii) internal densities of 2.7 g cm^{-3},
(iv) mean orbital eccentricities of 0.05 and inclinations of 1.4 deg ($i \sim e/2$) that set the relative velocities,
(v) an initial surface density of solids equivalent to a Minimum Mass Solar Nebula (MMSN) extrapolated out to 100 au ($\Sigma(r) = (r/1\text{ au})^{-1.5}\ M_\oplus\ \text{au}^{-2}$, Weidenschilling 1977; Hayashi 1981).

For more detail on assumptions of this model we direct the reader to Wyatt et al. (2011) and Marino et al. (2017). The output from these simulations are size distributions at different radii that we translate to surface densities or disc masses in mm-sized grains, here defined as all grains smaller than 1 cm. These mm-sized grains are what our ALMA observations are most sensitive to, since grains in the range 0.1–10 mm dominate the emission at these wavelengths and the mass of grains smaller than 1 cm. This choice is consistent with the dust opacity that is assumed to translate fluxes to dust masses (see below).

3.1 TRAPPIST-1 collisional evolution

Given the estimated age of 7.6±2.2 Gyr (Burgasser & Mamajek 2017), it is likely that any debris disc present around TRAPPIST-1 has suffered significant collisional evolution. This means that even if this system was born with a massive disc of planetesimals and detectable dust levels, after 8 Gyr of evolution it could have lost most of its mass through collisions and the removal of small dust subject to stellar winds and radiation pressure (although the latter is not high enough to remove grains larger than ~ 0.01 μm).

To quantify which initial planetesimal belt parameters are allowed by our non-detection, we derive an upper limit on the surface density and total mass of a collisionally produced dust disk by assuming:

(i) the belt is edge-on, i.e. co-planar to TRAPPIST-1 b–h,
(ii) a dust opacity of 3 cm^2 g^{-1} at 0.88 mm,

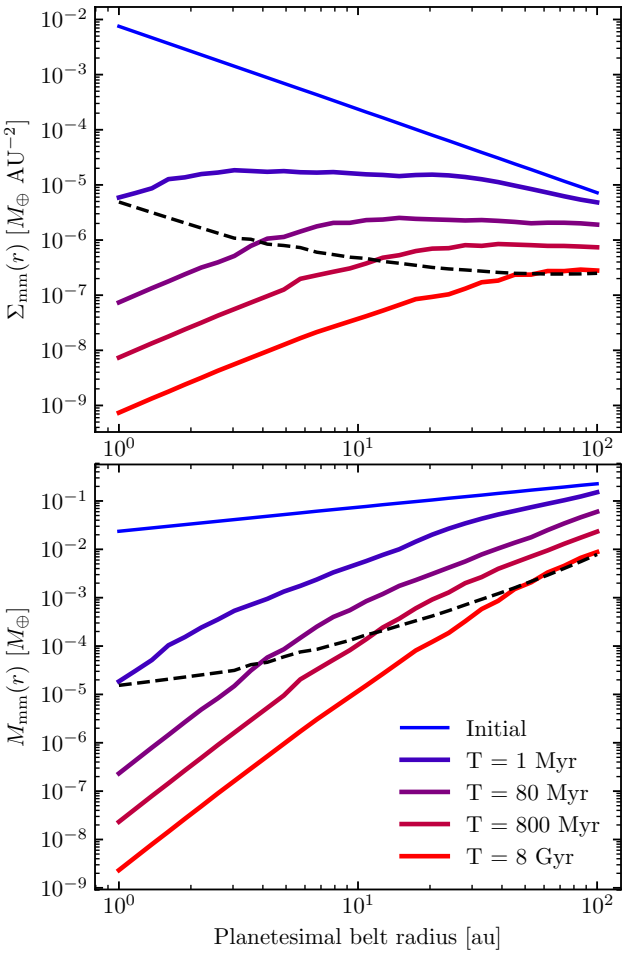

Figure 4. Collisional evolution of the surface density (top) and belt mass (bottom) in mm-sized grains around TRAPPIST-1, as a function of radius and time (continuous colour lines). As a comparison, the dashed line shows the ALMA upper limit derived in this work. The upper limit for the surface density is derived assuming a belt fractional width of 0.5 and an edge-on orientation (i.e., the dashed line shows the limit on the surface density of a belt at that radius, rather than the limit on the surface density of an extended disk at that radius).

(iii) equilibrium blackbody temperatures in the optically thin regime (considering both the stellar radiation and ISRF),
(iv) a belt width that is half of the belt central radius (typical of debris discs, Matrà et al. 2018b).

The adopted dust opacity is consistent with the one expected for grains smaller than 1 cm in a size distribution according to our collisional evolution model, i.e. $N(a) \sim a^{-3.4}$ in the range 10 μm—100 m (Woitke et al. 2016).

Figure 4 compares the predicted surface density (top) and disc mass in mm-sized grains at different epochs (continuous lines) with the 3σ upper limit derived by our observations (dashed lines). Note that our upper limits for the surface density do not correspond to expected disc profiles, but rather the maximum surface density if the planetesimal belt was centred at that radius and had a fractional width (width over central radius) of 0.5. Beyond 40 au, our model predicts

dust levels that would be detectable. Therefore we conclude that our observations rule-out that TRAPPIST-1 was born with a planetesimal belt of mass similar to or larger than a MMSN ($\gtrsim 20\ M_\oplus$) at a radius between 40–100 au. If we take the mass and orbits of TRAPPIST-1 planets derived by Grimm et al. (2018) we find a *minimum mass TRAPPIST-1 nebula* that is $\Sigma = 670 \pm 40(r/0.02\ \mathrm{au})^{-1.8\pm0.1}\ M_\oplus\ \mathrm{au}^{-2}$. This expression extrapolated to large radii translates into surface densities lower than assumed in our model and thus consistent with our non-detection. Note that this approach to derive an initial mass in solids assumes planets' orbits do not evolve significantly, which might not be the case for TRAPPIST-1 planets (Ormel et al. 2017; Schoonenberg et al. 2019). Moreover, extrapolating the relationship of stellar luminosity and belt radius found by Matrà et al. (2018a) to TRAPPIST-1's luminosity, we do not expect a belt radius larger than 25 au. Interior to 40 au, our upper limit is significantly higher than the predicted dust levels after 8 Gyr of evolution, hence collisional evolution alone can explain our disc non-detection, and thus a planetesimal disc more massive than a MMSN could have formed there when this system formed. Note that interior to 40 au this system could still host a MMSN-like planetesimal disc but that is faint today due to how the size distribution has evolved, with the mass in small bodies orders of magnitude more depleted than the mass in the largest bodies (Schüppler et al. 2016; Marino et al. 2017).

These conclusions hold when varying model parameters such as the maximum planetesimal size and level of stirring since the surface density of mm-sized grains in collisional equilibrium is not very sensitive to these (see Equation 3 in Marino et al. 2019). Other assumptions to translate flux upper limits to surface densities could have a small effect. For example, assuming the belt is wider would distribute roughly the same dust mass upper limit (or flux upper limit) over a larger area, and thus it would lower our upper limit on the surface density derived from observations. Only by decreasing the initial surface density of solids in our collisional model or narrowing the assumed belt, the predicted surface density of mm-sized dust would be lower than our upper limit at all radii. A caveat in the use of our collisional evolution model is that it assumes the system has been stable for 8 Gyr. The non-detection of a disc could also be explained by an instability in the system that scattered and depleted a massive planetesimal belt.

3.2 Proxima Cen collisional evolution

We applied the same model to Proxima Cen (age of ~ 5 Gyr, Bazot et al. 2016) which hosts a low mass temperate planet (Anglada-Escudé et al. 2016) and has also been observed by ALMA at 1.3 mm. To derive upper limits we re-imaged the data after applying the calibration script provided by ALMA. In the original analysis of the data by Anglada et al. (2017), they proposed the existence of warm dust component at 0.4 au, a cold belt at 1–4 au and an outer belt at 30 au. An independent analysis by MacGregor et al. (2018) of the same observations showed that in the same ALMA data there is strong and time variable flaring activity from Proxima Cen. This time-variable and unresolved emission could have misled Anglada et al. (2017) to conclude that there is circumstellar dust within a few au. Moreover, the signal from the putative outer belt after azimuthally averaging (as in Marino et al. 2016) is only marginally significant at 3.5σ. A future detailed analysis of more sensitive observations in the visibility space, taking into account the time variable emission of Proxima Cen, should be able to confirm or rule out the presence of dust emission in this system at the levels claimed by Anglada et al. (2017).

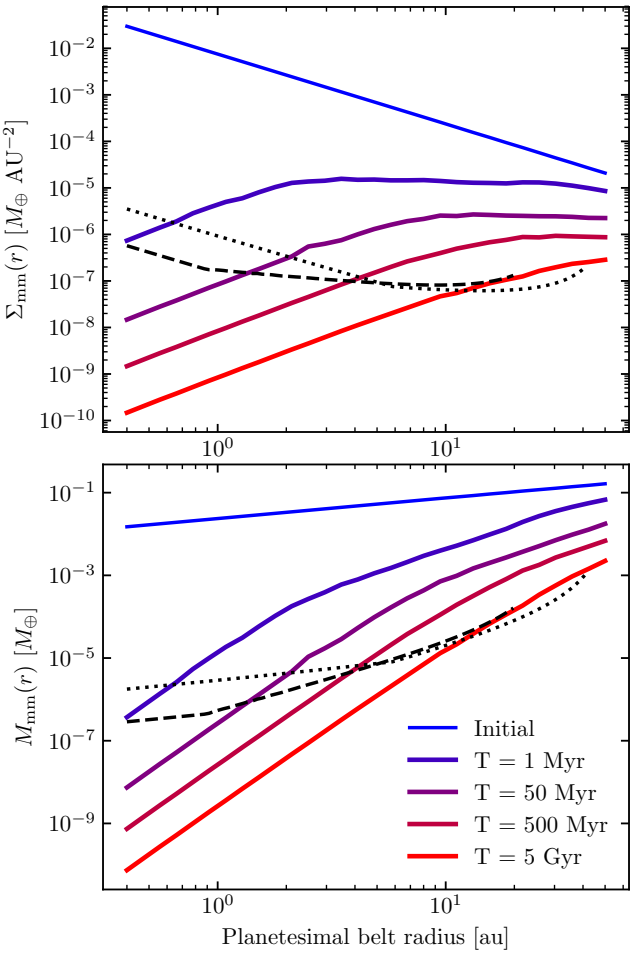

Figure 5. Collisional evolution of the surface density (top) and belt mass (bottom) in mm-sized grains around Proxima Cen, as a function of radius and time (continuous colour lines). As a comparison, the dashed and dotted lines show the ALMA upper limit derived using the 12m+ACA and ACA alone images, respectively. The upper limit for the surface density is derived assuming a belt fractional width of 0.5 and a belt inclination of 45 deg as suggested by Anglada et al. (2017).

Despite this ongoing debate on the presence of debris-like dust around Proxima Cen, in Figure 5 we compare the results from collisional evolution with the upper limits from the ACA map (dotted line) and 12m and ACA combined (dashed line) assuming a disc inclined by 45 deg and azimuthally averaging. We find that the ACA observations could have marginally detected a disc if it had a mean radius between 10–40 au and was as massive as a MMSN (10–20 $M_\oplus$) under the assumptions stated above. This mass however is not well constrained since interior to 40 au the whole size distribution is in collisional equilibrium (proved by the

constant slope of $r^{7/3}$ in the model surface density, Wyatt 2008; Kennedy & Wyatt 2010). This means that even if the belt had started with a larger mass it would have depleted faster reaching the same mass after 5 Gyr. By varying the initial disc mass we find that discs with a mass lower than a tenth of a MMSN would have a surface density below the detection limit (at ~ 30 au). Therefore, we conclude that the amount of mm-sized dust in the putative outer belt around Proxima Cen is not unrealistic, and roughly consistent with the collisional evolution of a planetesimal belt that was born with a tenth of a MMSN (1–2 $M_\oplus$).

3.3 Searching for debris-like dust around low mass stars

In this paper we have shown how important collisional evolution is when interpreting upper limits on the presence of dust around low mass stars. At tens of au, the dust mass is expected to decrease with age roughly as $t^{-0.4}$ while the lifetime of the largest planetesimals is longer than the age of the system, and t^{-1} at later times (e.g. Löhne et al. 2008). Thus, the age of surveyed systems is a key factor to consider when selecting targets to observe. In addition to this, the distance to the source is very important too since the flux is inversely proportional to the distance squared. Proof of this is that the sensitivities or upper limits on the dust mass around Proxima Cen are ~ 5 times better than for TRAPPIST-1, even though the noise in the reconstructed images was poorer. Future searches should take into account both age and distance to be the most sensitive to debris-like dust. Therefore, we recommend then that surveyed samples should be composed of young and nearby systems that are expected to have the largest flux, i.e. that minimise the quantity $t^{0.4}d^2$ if the largest planetesimals are not yet in collisional equilibrium ($r > r_c$ in Equation 8 from Marino et al. 2017), or td^2 if they are ($r < r_c$).

4 SUMMARY AND CONCLUSIONS

In this paper we have reported new ALMA observations around TRAPPIST-1 at 0.88 mm, the deepest to search for dust emission from a debris disc around this system. These observations did not detect circumstellar dust or CO 3-2 emission. We compared our dust upper limits with collisional evolution models, which given TRAPPIST-1's age of ~ 8 Gyr predict detectable dust levels beyond 40 au if the initial disc was as massive as a MMSN. Therefore our model rules-out that TRAPPIST-1 was born with a planetesimal belt larger than 40 au and with a mass similar or higher than a MMSN ($\gtrsim 20\ M_\oplus$). Within 40 au, on the other hand, the surface density or total mass of mm-sized dust could be simply depleted due to collisional evolution and avoid detection. The solid mass upper limit derived here is comparable to the mass in TRAPPIST-1 planets ($\sim 5.7\ M_\oplus$, Grimm et al. 2018), thus it possible that most of the available solid mass in these systems was transported inwards and used to form the known planets.

We searched in time bins of 12s for any flaring activity of TRAPPIST-1 that could be present in this data. We did not find any significant emission, and we derive a 5σ upper limit of 1.2 mJy for variable emission over 12s windows.

Given the available archival ALMA data on Proxima Cen, also a system around a low mass star hosting a low mass temperate planet, we performed a similar analysis. We compared our model with ALMA observations and showed that the current upper limits are slightly below the mass of mm-sized dust that we expect given our collisional evolution model. The archival observations could have marginally detected a belt with a mean radius between 10–40 au and with an initial mass $\gtrsim 1\ M_\oplus$. This means that the marginal detection of an outer belt at 30 au by Anglada et al. (2017) is consistent with our collisional evolution model and a belt that was born with a tenth of a MMSN. An even more massive disc would have collisionally evolved to the same mass and thus these observations cannot constrain well the initial mass of a putative planetesimal belt. Interior to 10 au, the limits cannot rule out that the system was born with a planetesimal belt more massive than a MMSN.

We conclude that in order to set tighter constraints on planetesimal discs around low mass stars with planets, we should focus most efforts on nearby and, if possible, young ($\lesssim 1$ Gyr old) systems. Nearby systems ensure a higher flux with a strong dependence on the distance, while younger systems are also more likely to host not yet collisionally depleted belts beyond a few au. In §3.3 we showed how the flux depends more strongly on the distance, and how both distance and age can be taken into account when prioritising which targets to observe. Such systems could provide important constraints to the formation of planetary systems around low mass stars.

ACKNOWLEDGEMENTS

GMK is supported by the Royal Society as a Royal Society University Research Fellow. LM acknowledges support from the Smithsonian Institution as a Submillimeter Array (SMA) Fellow. MK gratefully acknowledges funding from the European Union's Horizon 2020 research and innovation programme under the Marie Sklodowska-Curie Fellowship grant agreement No 753799. T.H. acknowledges support from the European Research Council under the Horizon 2020 Framework Program via the ERC Advanced Grant Origins 83 24 28. This paper makes use of the following ALMA data: ADS/JAO.ALMA#2017.1.00215.S and ADS/JAO.ALMA#2016.A.00013.S. ALMA is a partnership of ESO (representing its member states), NSF (USA) and NINS (Japan), together with NRC (Canada), MOST and ASIAA (Taiwan), and KASI (Republic of Korea), in cooperation with the Republic of Chile. The Joint ALMA Observatory is operated by ESO, AUI/NRAO and NAOJ.

REFERENCES

Anglada-Escudé G., et al., 2016, Nature, 536, 437
Anglada G., et al., 2017, ApJ, 850, L6
Aravena M., et al., 2016, ApJ, 833, 68
Bazot M., Christensen-Dalsgaard J., Gizon L., Benomar O., 2016, MNRAS, 460, 1254
Benz W., Asphaug E., 1999, Icarus, 142, 5
Binks A. S., Jeffries R. D., 2017, MNRAS, 469, 579
Burdanov A. Y., et al., 2019, MNRAS, 487, 1634
Burgasser A. J., Mamajek E. E., 2017, ApJ, 845, 110

Carniani S., et al., 2015, A&A, 584, A78
Cresswell P., Nelson R. P., 2006, A&A, 450, 833
Dencs Z., Regály Z., 2019, MNRAS, 487, 2191
Dorn C., Mosegaard K., Grimm S. L., Alibert Y., 2018, ApJ, 865, 20
Eiroa C., et al., 2013, A&A, 555, A11
Filippazzo J. C., Rice E. L., Faherty J., Cruz K. L., Van Gordon M. M., Looper D. L., 2015, ApJ, 810, 158
Gautier III T. N., et al., 2007, ApJ, 667, 527
Gillon M., et al., 2016, Nature, 533, 221
Gillon M., et al., 2017, Nature, 542, 456
Grimm S. L., et al., 2018, A&A, 613, A68
Hansen B. M. S., Murray N., 2012, ApJ, 751, 158
Hardegree-Ullman K. K., Cushing M. C., Muirhead P. S., Christiansen J. L., 2019, AJ, 158, 75
Hayashi C., 1981, Progress of Theoretical Physics Supplement, 70, 35
Hughes A. M., Duchêne G., Matthews B. C., 2018, ARA&A, 56, 541
Hughes A. G., Boley A. C., Osten R. A., White J. A., 2019, ApJ, 881, 33
Kennedy G. M., Wyatt M. C., 2010, MNRAS, 405, 1253
Kennedy G. M., et al., 2018, MNRAS, 476, 4584
Kral Q., Wyatt M. C., Triaud A. H. M. J., Marino S., Thébault P., Shorttle O., 2018, MNRAS, 479, 2649
Krivov A. V., 2010, Research in Astronomy and Astrophysics, 10, 383
Lestrade J. F., Wyatt M. C., Bertoldi F., Menten K. M., Labaigt G., 2009, A&A, 506, 1455
Li A., Draine B. T., 2001, ApJ, 554, 778
Löhne T., Krivov A. V., Rodmann J., 2008, ApJ, 673, 1123
Luger R., et al., 2017, Nature Astronomy, 1, 0129
MacGregor M. A., Weinberger A. J., Wilner D. J., Kowalski A. F., Cranmer S. R., 2018, ApJ, 855, L2
Marino S., et al., 2016, MNRAS, 460, 2933
Marino S., Wyatt M. C., Kennedy G. M., Holland W., Matrà L., Shannon A., Ivison R. J., 2017, MNRAS, 469, 3518
Marino S., Bonsor A., Wyatt M. C., Kral Q., 2018, MNRAS, 479, 1651
Marino S., Yelverton B., Booth M., Faramaz V., Kennedy G. M., Matrà L., Wyatt M. C., 2019, MNRAS, 484, 1257
Mathis J. S., Mezger P. G., Panagia N., 1983, A&A, 500, 259
Matrà L., Wilner D. J., Öberg K. I., Andrews S. M., Loomis R. A., Wyatt M. C., Dent W. R. F., 2018a, ApJ, 853, 147
Matrà L., Marino S., Kennedy G. M., Wyatt M. C., Öberg K. I., Wilner D. J., 2018b, ApJ, 859, 72
Matthews B. C., Krivov A. V., Wyatt M. C., Bryden G., Eiroa C., 2014, Protostars and Planets VI, pp 521–544
Mezger P. G., Mathis J. S., Panagia N., 1982, A&A, 105, 372
Montesinos B., et al., 2016, A&A, 593, A51
Moran S. E., Hörst S. M., Batalha N. E., Lewis N. K., Wakeford H. R., 2018, AJ, 156, 252
Mulders G. D., Pascucci I., Apai D., 2015, ApJ, 814, 130
O'Malley-James J. T., Kaltenegger L., 2017, MNRAS, 469, L26
Ormel C. W., Liu B., Schoonenberg D., 2017, A&A, 604, A1
Plavchan P., Jura M., Lipscy S. J., 2005, ApJ, 631, 1161
Schoonenberg D., Liu B., Ormel C. W., Dorn C., 2019, A&A, 627, A149
Schüppler C., Krivov A. V., Löhne T., Booth M., Kirchschlager F., Wolf S., 2016, MNRAS, 461, 2146
Schwarz R., et al., 2018, MNRAS, 480, 3595
Sibthorpe B., Kennedy G. M., Wyatt M. C., Lestrade J. F., Greaves J. S., Matthews B. C., Duchêne G., 2018, MNRAS, 475, 3046
Simpson J. M., et al., 2015, ApJ, 807, 128
Stewart S. T., Leinhardt Z. M., 2009, ApJ, 691, L133
Terquem C., Papaloizou J. C. B., 2007, ApJ, 654, 1110
Wakeford H. R., et al., 2019, AJ, 157, 11
Weidenschilling S. J., 1977, Ap&SS, 51, 153
Woitke P., et al., 2016, A&A, 586, A103
Wright E. L., et al., 2010, AJ, 140, 1868
Wyatt M. C., 2008, ARA&A, 46, 339
Wyatt M. C., Clarke C. J., Booth M., 2011, Celestial Mechanics and Dynamical Astronomy, 111, 1
de Wit J., et al., 2016, Nature, 537, 69
de Wit J., et al., 2018, Nature Astronomy, 2, 214

This paper has been typeset from a TEX/LATEX file prepared by the author.